Evolution of triaxial shapes at large isospin: Rh isotopes

A. Navin [a,*], M. Rejmund [a], S. Bhattacharyya [b], R. Palit [c], G.H. Bhat [d], J.A. Sheikh [d],
A. Lemasson [a], S. Bhattacharya [b], M. Caamaño [e], E. Clément [a], O. Delaune [a], F. Farget [a],
G. de France [a], B. Jacquot [a]

[a] GANIL, CEA/DRF – CNRS/IN2P3, Bd Henri Becquerel, BP 55027, F-14076 Caen Cedex 5, France
[b] Variable Energy Cyclotron Centre, 1/AF Bidhan Nagar, Kolkata 700064, India
[c] Department of Nuclear and Atomic Physics, Tata Institute of Fundamental Research, Colaba, Mumbai, 400 005, India
[d] Department of Physics, University of Kashmir, Srinagar, 190 006, India
[e] USC, Universidad de Santiago de Compostela, E-15706 Santiago de Compostela, Spain

ARTICLE INFO

ABSTRACT

The rotational response as a function of neutron–proton asymmetry for the very neutron-rich isotopes of Rh ($^{116–119}$Rh) has been obtained from the measurement of prompt γ rays from isotopically identified fragments, produced in fission reactions at energies around the Coulomb barrier. The measured energy "signature" splitting of the yrast bands, when compared with the Triaxial Projected Shell Model (TPSM) calculations, shows the need for large, nearly constant, triaxial deformations. The present results are compared with global predictions for the existence of non axial shapes in the periodic table in the case of very neutron-rich nuclei Rh isotopes. The predicted trend of a second local maximum for a triaxial shape around $N \sim 74$ is not found.

A basic property of atomic nuclei is its shape, which governs its various static as well as dynamic properties, and depends on the interaction among its constituents (Z protons and N neutrons). Shapes ranging from spherical to tetrahedral are predicted across the nuclear landscape. The evolution of nuclear shapes as a function of angular momentum and isospin is of prime importance in nuclear structure studies [1,2]. There is a predominance of prolate over oblate shapes for the ground state of even-Z even-N axially deformed nuclei [3]. Deviations from axial symmetry and the existence of triaxial "rigidly deformed" nuclei, first predicted in the late 50's, were assumed to be commonly possible [4,5]. There have been a sustained experimental and theoretical efforts to establish the signature of triaxial shapes of nuclei of various mass regions. Most of these nuclei were found to exhibit vibrational modes or "softness" with respect to the triaxiality parameter γ [6–8]. In the odd-A nuclei near $A \sim 190$ evidence of asymmetric shapes have been suggested from the comparison of the measured high spin levels with calculations based on a model of asymmetric rotor coupled to nucleon in a single-j orbital [9]. For a model independent measure of triaxiality, the cubic shape parameter analysis was used

to establish maximum effective large triaxiality for certain isotopes of Os and Pt [10]. Multiple Coulomb excitation studies have been used to study the breaking of axial symmetry [11]. Data on the splitting of the iso-vector GDR in certain nuclei was also shown to be sensitive to the deformation and triaxiality [12]. The rotation of triaxial nuclei has been suggested to be manifested as chiral partner bands [13], which initiated several experimental investigations [14–16] in recent years.

Möller et al. [17] made a systematic study to investigate the sensitivity of the ground-state nuclear masses with the inclusion of axial asymmetry, for nuclei both near and far from stability. They showed the correlation between the need for axial asymmetry and the presence of experimentally known characteristic γ-bands in nuclei around stability. For these nuclei, a systematic deviation between the calculated and the measured masses was removed by the inclusion of axial asymmetry. This study gave a surprisingly small number of nuclei (~ 70 out of 3000) whose calculated masses were affected by axial-symmetry breaking. These calculations showed that the effect of axial asymmetry is maximum around $Z = 44$, $N = 64$ and also predicted another additional region of increased triaxiality around $N \sim 74$ for these elements. However in this region, systematic beyond mean field calculations, for even–even nuclei, using the Gogny D1S interaction, extended by a 5-Dimensional Collective Hamiltonian (5DCH), predict

a smooth evolution of γ for the relevant isotopes but with a decreasing mean value of the quadrupole deformation [18]. Thus the measurements of very neutron-rich Ru and Rh isotopes are important to probe the evolution of triaxiality very far from stability. These isotopes are interesting candidates to probe whether the relevant excited states and their decay patterns provide a signature of triaxiality. This could also help in establishing the link between the lowering of ground state masses when axial symmetry is broken to pattern of excited states that are uniquely related to triaxial shape. Calculations relating nuclear masses to collective structures have also been reported [19].

The energies of excited states as a function of angular momenta provide an experimental handle to identify triaxial shapes. The signature quantum number is associated with the invariance of the intrinsic Hamiltonian of an axially-deformed nucleus with respect to 180° rotation around a principal axis. A signature-dependent term implies that rotational bands with $K \neq 0$ (K is the angular momentum projection of the quasi particles along the symmetry axis), in a system with rotational invariance, tend to separate into two groups, characterized by "favored" and "unfavored" signature quantum number [20]. The shift between these energetically favored and unfavored sequences of levels (energy signature splitting), is used to understand non-axial shapes in nuclei [21,22].

We report here on the spectroscopy of the high spin states in odd-Z Rh neutron-rich isotopes $^{116-119}$Rh, which could not be accessed earlier experimentally, to understand the evolution of nuclear triaxiality far from the valley of stability. These results are examined in the light of global predictions for triaxiality in the periodic table. It is important to note that the earlier investigations [10–12] provide experimental evidence for triaxiality of nuclei, some of which are in variance with the prediction of the finite range liquid drop model (FRLDM) [17].

The measurements were performed at GANIL using a ^{238}U beam at 6.2 MeV/u (~ 0.2 pnA) on a 10-micron thick ^{9}Be target. The fission fragments were identified in mass number (A) and atomic number (Z) in the VAMOS++ spectrometer [23] placed at 20° with respect to the beam axis. The time of flight was obtained from two multi wire parallel plate avalanche counters MWPPACs, one located after the target and the other at the focal plane (flight path ~ 7.5 m). The various measured positions, energies, and times, along with the known magnetic field, were used to determine, on an event-by-event basis, A, charge state (q), Z, and the velocity vector ($\vec{v}$) for the detected fragment [23]. The prompt γ rays were measured in coincidence with these isotopically identified fragments using the EXOGAM array [24], which consisted of 11 Compton-suppressed segmented clover HPGe detectors placed 15 cm from the target. The γ-ray energies of the fragments in their rest frame were obtained from the measured $\vec{v}$ along with the known angle of the segment of the relevant clover detector [23, 25]. More details of the method and measurement can be found in Ref. [26,27]

Fig. 1 shows the γ-ray spectra for the isotopically identified $^{114-119}$Rh isotopes measured in this work. The derived level schemes for $^{114-119}$Rh obtained using $\gamma - \gamma$ coincidences, energy sums, and relative intensities, are shown in Fig. 2 and Fig. 3 for the odd-A and even-A Rh isotopes respectively. The resulting level schemes extracted for ^{114,115}Rh confirm those previously obtained in literature [28,29], including those for the side bands (not shown in Fig. 2). Additionally, the 255.2 keV and 774.9 keV transitions corresponding to the side bands of ^{114}Rh and ^{115}Rh respectively and the 215.5 keV transition of the main band in ^{115}Rh were placed from the present measurement. A few more new transitions were also seen in the mass gated spectra but could not be placed in the level scheme due to lack of sufficient statistics for $\gamma - \gamma$ correlations for these transitions. A comparison with
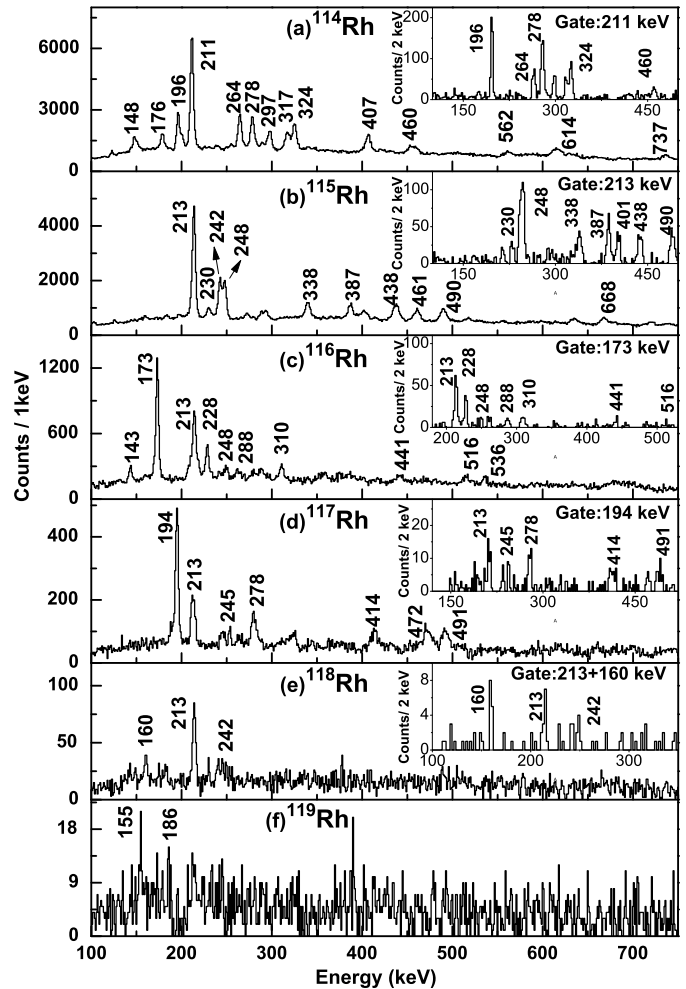

Fig. 1. *A*- and *Z*-identified Doppler-corrected γ-ray spectra for the $^{114-119}$Rh isotopes. The insets in the respective panels shows the $\gamma - \gamma$ coincidence spectra.

other known lighter even-A Rh isotopes suggests that the 143.4 and 310.7 keV transitions in ^{116}Rh (Fig. 1c) could belong to a side band. The spin-parities are proposed based on the systematics of the known schemes of the lower-A Rh isotopes [30]. In ^{114}Rh, a high spin 7^- isomer [31] and in ^{116}Rh [32] a 6^- isomer were tentatively suggested. A similar isomer with $J > 4$ was proposed in ^{118}Rh [33]. No coincidences were possible for ^{119}Rh due to the low statistics in this very exotic nucleus. The γ rays for $^{116-119}$Rh are reported for the first time (a single transition from the decay of a low spin isomeric decay state has been earlier reported in ^{117}Rh [34]). Detection of the prompt γ rays in the Rh isotopic chain up to $N/Z = 1.64$, $N = 74$, (as compared to $N = 70$ obtained from the traditional high-fold γ coincidence method), was only possible because of the increased sensitivity and selectivity of the present setup.

The quantum mechanical triaxial projected shell model (TPSM) is used to understand the band structure and signature splitting of the neutron-rich Rh isotopes. Various phenomena related to triaxial shapes of nuclei, like γ-vibrations [35], chiral symmetry [36, 37], and wobbling modes [38], have been successfully described using the TPSM. More recently, the TPSM along with Density Functional Theory (DFT) provided a consistent description of data for even–even nuclei near ^{110}Ru [39]. In the TPSM, the quasi-particle states are generated by solving the triaxial Nilsson and pairing (monopole and quadrupole terms) Hamiltonian in the BCS approximation [35,37,40,41] with the relevant deformation parameters,
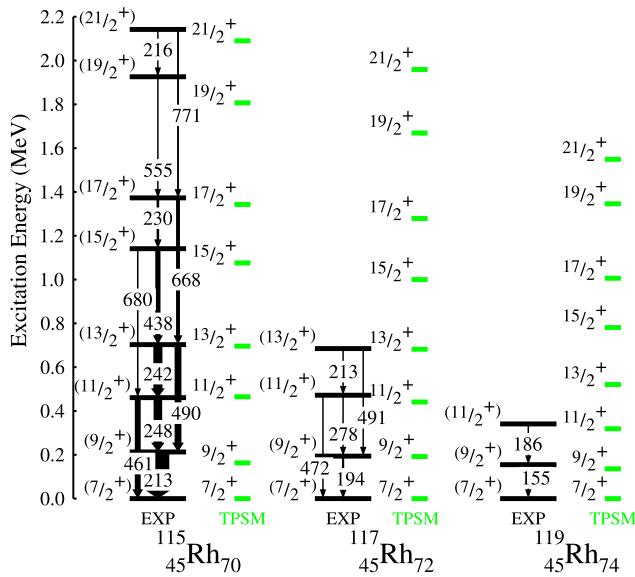
Fig. 2. Yrast bands of odd-*A* isotopes of Rh built on the low-energy high-spin states studied in this work. Excitation energies (in keV) are relative to the $7/2^+$ levels. The corresponding TPSM calculations are also shown (see text).


Fig. 3. Yrast bands of even-*A* isotopes of Rh built on the low-energy high-spin states studied in this work. Excitation energies (in keV) are relative to the 7^- levels. The corresponding TPSM calculations are also shown including a low lying excited band (see text).

ϵ and ϵ' ($\gamma = tan^{-1}(\epsilon'/\epsilon)$). To obtain the states in the laboratory frame, the broken rotational symmetries in these deformed multi-quasi-particle states are projected onto good angular-momentum states through a three-dimensional angular momentum projection formalism. Each triaxial configuration is composed of several K values and the corresponding bands are obtained by assigning a given K value in the angular momentum projection operator [40]. These projected basis states are then employed to diagonalize the shell model Hamiltonian. The final states so obtained, because of the configuration mixing (different K values), do not have a well defined K quantum number. The triaxial configuration, in the case of an even-Z–even-N system, is an admixture of different K states and the vacuum configuration is composed of $K = 0, 2, 4, \ldots$ states [40–42]. The details of the formalism for odd-Z–even-N and odd-Z–odd-N nuclei can be found in Refs. [35,37].

For the Rh isotopes discussed here, three major shells, $N = 3, 4$ and 5 (2, 3 and 4) for neutrons (protons), were used in the calculation. In the case of the odd-*A* Rh isotopes, the one-quasi-particle configuration ($1-qpc$) (proton) and three-quasi-particle configurations ($3-qpc$) (one-proton and two-neutrons) were used to compute the states measured in the present work. Similarly, for the even-*A* Rh isotopes, the two-quasi-particle configurations ($2-qpc$) (one proton and one neutron) were generated using the same method. The calculations used a standard set of parameters for this mass region [36]. In the present work, the values of ϵ and ϵ' were adopted so that experimental data is reproduced reasonably well. The ϵ value chosen in the TPSM analysis is close to those obtained in mean-field calculations [43], however, deviations were noted for ϵ'. In should be noted that in the TPSM approach, the basis states are generated by solving the Nilsson potential with the input deformation values of ϵ and ϵ', and these deformation values also fix the strength of the quadrupole-quadrupole part of the Hamiltonian through self-consistency conditions. However, the final deformation (quadrupole moment) calculated using the projected wavefunctions may be different from the input deformation used for the bases. The reason is that the Hamiltonian is diagonalized using the projected multi-quasiparticle basis states and many-body correlations entering though this process can alter initial deformation values.
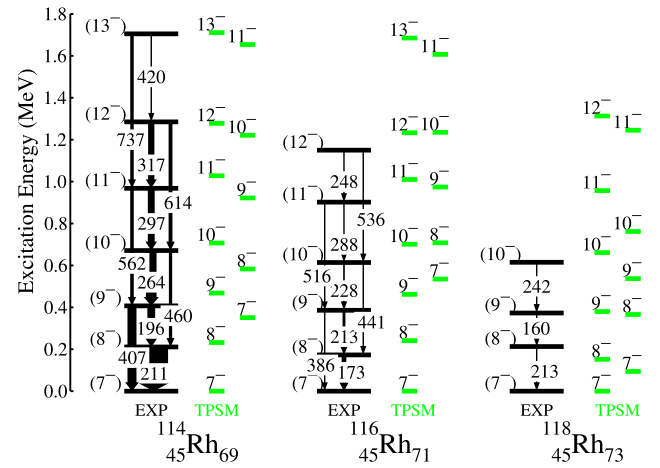
The projected energies for the different configurations before configuration mixing provide insights into the structure of the bands. The locus of the projected energies at various spins for a particular configuration is referred to as a band. We first describe the calculations (performed up to $I^\pi = 29/2^+$) for the odd-*A* Rh isotopes. The lowest band (ground) is found to be built on a $1-qpc$ with $K = 7/2$. At low spin, the next favorable band, which lies close to ground band, is the γ-band with $K = K_\gamma + 2$, K_γ being the K-value of the ground band. The other γ-band with $K = K_\gamma - 2$ is found to be energetically less favorable. For higher spin ($I^\pi \geq 15/2^+$), a $3-qpc$ with $K = 1/2$ is found to have an energy similar to the $1-qpc$ $K = 7/2$ and $K = 11/2$ band. After configuration mixing, the amplitudes (which vary as a function of the angular momentum) for the various components of the low lying yrast states are found to be dominated by the $K = 7/2$ component along with additional small components arising from the $K = 11/2$ and the $K = 1/2$ states. The energies obtained after diagonalization for the yrast band in the odd-A Rh isotopes are shown (using the deformation values given in Table 1) and are compared with the corresponding experimental data in Fig. 2. The figure shows that the TPSM calculations are able to describe the energies of the excited states well. The signature splitting at lower spin is found to arise from $K = 7/2$ states. The increase in the signature splitting at higher spin can be attributed to mixing of the $K = 1/2$ states. Fig. 4 illustrates the sensitivity of the calculations for the energy difference between consecutive spin levels (signature splitting) for various values of γ for ^{115,117}Rh. In the case of the calculations for the even-*A* Rh isotopes (performed up to $I^\pi = 18^-$), different $2-qpc$ with $K = 1, 3, 5, 7$ and 9 were considered (only odd-K configurations were used since they were energetically more favorable). The two bands having the lowest energy were found to be based on configurations with $K = 7$ and 9 respectively. Their excitation energies were found to be within 100 keV for the entire spin range. The calculated yrast states, obtained after band mixing were found to give an overall good description of the data and are shown in Fig. 3. Additionally, these calculations predict an excited band very close to the yrast band (see Fig. 3) and the energy difference between the ground and partner band is found to be minimum for ^{118}Rh. Challenging measurements of these excited bands which could be signature of chiral symmetry can be addressed with next generation γ-ray tracking detectors [44] coupled to a large spectrometer [23,45]. Fig. 5 illustrates the sensitivity of the calculations to various values of γ for ^{114,116,118}Rh. Fig. 4 and
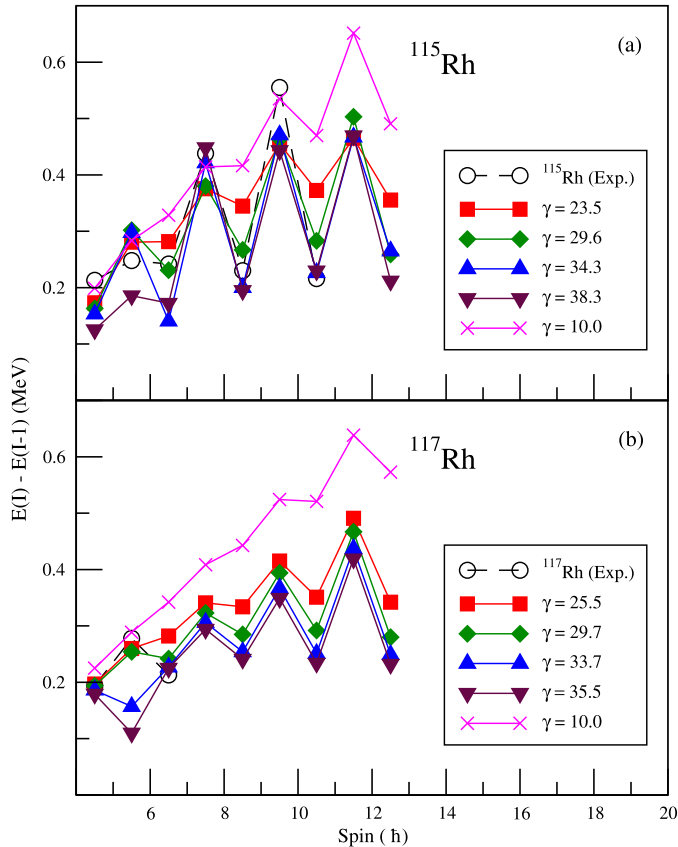
Fig. 4. Experimental energy signature splitting $(E(I) - E(I - 1))$ for (a) ^{115}Rh and (b) ^{117}Rh compared with the TPSM results for various triaxial deformation parameter γ.

Table 1
The axial deformation parameter (ϵ) and triaxial deformation parameter (ϵ') employed in the calculation for $^{114-119}$Rh isotopes $(\gamma = tan^{-1}(\epsilon'/\epsilon))$.

	^{114}Rh	^{115}Rh	^{116}Rh	^{117}Rh	^{118}Rh	^{119}Rh
ϵ	0.230	0.190	0.221	0.210	0.210	0.180
ϵ'	0.130	0.108	0.130	0.120	0.150	0.105
γ	29.5	29.6	30.5	29.7	35.5	30.3

Fig. 5 also illustrates the trend of signature splitting as a function of spin for the Rh isotopic chain, along with the corresponding calculations using the values which best describe the measurements (Table 1). It can be seen that the calculations reproduce well the measured signature splitting. The splitting is small at lower spin and increases with increasing spin. As shown in the Figs. 4 and 5, the calculated signature splitting with small triaxial deformation, say, $\gamma = 10$, has large deviation from the experimental values. It was also noted that the results for $\gamma = 0$ (not shown in the figure) is close to $\gamma = 10$.

The structure and the magnitude of signature splittings are now used to understand the degree of triaxiality in neutron-rich Rh isotopes. Fig. 6 demonstrates the need for large values of triaxial deformation (γ), shown in Table 1, to reproduce the signature splitting in neutron-rich Rh isotopes. The present work indicates that these neutron-rich nuclei have a similar trend for the signature splitting and the degree of triaxiality remains almost constant. The signature splitting for ^{115}Rh (^{114}Rh) was earlier reported in Ref. [28,29]; it was found to be similar to the lighter odd-*A* isotopes of Rh. As mentioned in the introduction, the analysis of Möller et al. [17] for the existence of non-axial shapes in the periodic table predicted a region of increased triaxiality around ^{119}Rh,
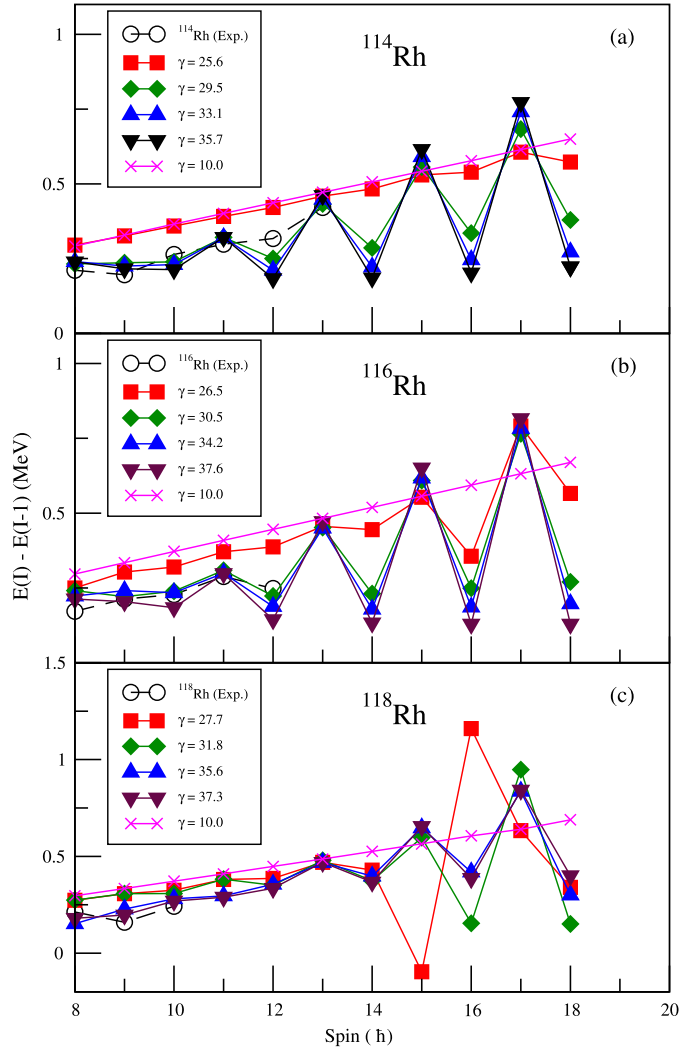
Fig. 5. Same as in Fig. 4 for the even-*A* isotopes (a) ^{114}Rh (b) ^{116}Rh and (c) ^{118}Rh.

in addition to the one known around ^{110}Rh. The current work presents the first comparison of these predictions with data for nuclei very far from stability. As can be seen from Table 1, the extracted triaxial deformations are nearly constant between ^{114}Rh and ^{119}Rh, and thus showing the absence of the existence of another region of increased triaxiality as predicted in Ref. [17]. The need for higher-order shape parameterization, which have been shown to be required in the actinide region [46] could be a possible reason for the discrepancy of Ref. [17] with the experimental results. Mean field calculations for even–even nuclei [47] predict changes in the S_{2n} near N ∼ 74 around Ru. Beyond mean field calculations of Ref. [18] predict a smooth evolution of γ for Ru and Pd but with a decreasing mean value of β. However Ref. [48] mentions that the mean values of β and γ deformation parameters obtained with 5-DCH calculations have to be taken with caution, and that small values of β imply almost no deformation and thus little relevance of the parameter γ. Thus these 5DCH calculations using the Gogny HFB mean field predict a vanishing of deformation and triaxiality for these nuclei [48]. Hence the present work shows the importance for such measurements for nuclei far from the valley of stability and points towards the need for improvements in the various predictions of triaxiality in this region. The evolution of these deformations could have an impact on the inputs required for calculating the abundance of elements in this mass region [49].
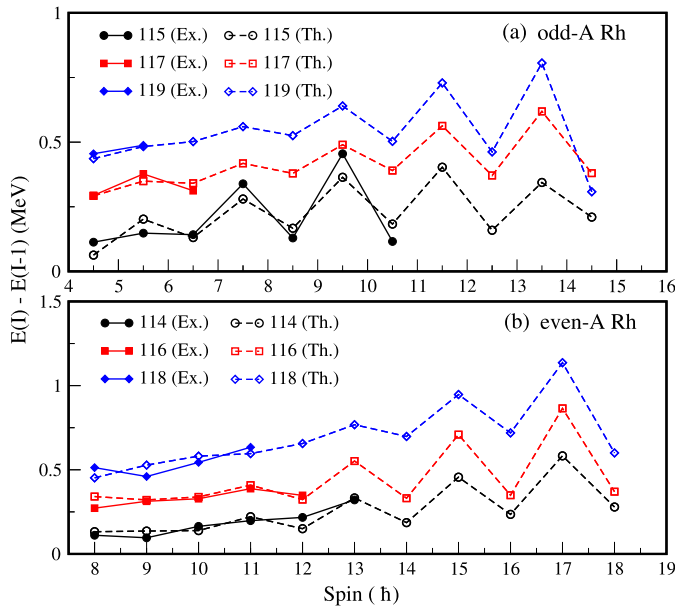
Fig. 6. Experimental and calculated signature splitting (with γ-deformation given in Table 1) for ^{115,117,119}Rh (a) and ^{114,116,118}Rh (b). For display purposes, the data and calculation are shifted by -100 keV, 100 keV, and 300 keV for ^{115}Rh (^{114}Rh), ^{117}Rh (^{116}Rh), and ^{119}Rh (^{118}Rh) respectively.

In summary, we have reported for the first time the rotational response, obtained from the measurement of prompt γ rays, of the very neutron rich isotopes of $^{116-119}$Rh. The calculations of the quantum mechanical model TPSM shows that the observed level energy differences are sensitive to the γ deformation for $^{116-119}$Rh isotopes, even at low spin. Using the TPSM results, the need for substantial and nearly constant triaxial deformation to explain the measured energy spectra for yrast bands is shown for the even-mass Rh as well as odd-mass Rh isotopes beyond ^{114}Rh and ^{115}Rh respectively. This work shows that evolution of triaxiality as a function of neutron number for the very neutron rich Rh isotopes differs from the global predictions for the evolution of non-axial shapes in the periodic table. In particular, for the predicted trend of a second local maxima for a triaxial shape around $N \sim 74$ is not observed. The present work is a first step in understanding the evolution of triaxial shapes far from stability. Further improvements in the experimental sensitivities, to be achieved in both fragment and γ-ray detection capabilities at energies around the Coulomb barrier, could allow the characterization of the non-yrast states in these nuclei to search for the presence of novel collective modes associated with the triaxial rotation, like chiral bands.

References

[1] X. Wang, M.A. Riley, J. Simpson, E.S. Paul, McGraw-Hill Yearbook of Science & Technology, 2013, p. 119.
[2] A.N. Andreyev, et al., Nature 405 (2000) 430.
[3] I. Hamamoto, Phys. Rev. C 89 (2014) 057301;
I. Hamamoto, B.R. Mottelson, Phys. Rev. C 79 (2009) 034317.
[4] A.S. Davydov, G.F. Filippov, Nucl. Phys. 8 (1958) 237.
[5] L. Wilets, M. Jean, Phys. Rev. 102 (1956) 788.
[6] N.V. Zamfir, R.F. Casten, Phys. Lett. B 260 (1991) 265.
[7] Y. Toh, et al., Phys. Rev. C 87 (2013) 041304(R).
[8] E.A. McCutchan, et al., Phys. Rev. C 76 (2007) 024306.
[9] J. Meyer-ter-Vehn, et al., Phys. Rev. Lett. 32 (1974) 383.
[10] V. Werner, et al., Phys. Rev. C 71 (2005) 054314.
[11] D. Cline, Annu. Rev. Nucl. Part. Sci. 36 (1986) 683.
[12] A.R. Junghans, et al., J. Korean Phys. Soc. 59 (2010) 1872.
[13] V.I. Dimitrov, S. Frauendorf, F. Donau, Phys. Rev. Lett. 84 (2000) 5732;
S. Frauendorf, J. Meng, Nucl. Phys. A 617 (1997) 131.
[14] K. Starosta, et al., Phys. Rev. Lett. 86 (2001) 971.
[15] P. Joshi, et al., Phys. Lett. B 595 (2004) 135.
[16] I. Kuti, et al., Phys. Rev. Lett. 113 (2014) 032501.
[17] P. Möller, et al., Phys. Rev. Lett. 97 (2006) 162502.
[18] J.-P. Delaroche, et al., Phys. Rev. C 81 (2010) 014303;
http://www-phynu.cea.fr/science_en_ligne/carte_potentiels_microscopiques/carte_potentiel_nucleaire_eng.htm.
[19] R.B. Cakirili, et al., Phys. Rev. Lett. 102 (2009) 082501.
[20] Aage Bohr, Ben R. Mottelson, Nuclear Structure, vol. II, W.A. Benjamin, Inc., Reading, Massachusetts, 1975.
[21] R. Bengtsson, H. Frisk, F.R. May, J.A. Pinston, Nucl. Phys. A 415 (1984) 189.
[22] I. Hamamoto, Phys. Lett. B 235 (1990) 221.
[23] M. Rejmund, et al., Nucl. Instrum. Methods Phys. Res. A 646 (2011) 184;
S. Pullanhiotan, et al., Nucl. Instrum. Methods A 593 (2008) 343.
[24] J. Simpson, et al., Acta Phys. Hung., Heavy Ion Phys. 11 (2000) 159.
[25] S. Bhattacharyya, et al., Phys. Rev. Lett. 101 (2008) 032501.
[26] A. Navin, M. Rejmund, McGraw-Hill Yearbook of Science & Technology, 2014, p. 137.
[27] A. Navin, et al., Phys. Lett. B 728 (2014) 136.
[28] S.H. Liu, et al., Phys. Rev. C 83 (2011) 064310.
[29] S.H. Liu, et al., Phys. Rev. C 84 (2011) 014304.
[30] Y.X. Luo, et al., Phys. Rev. C 69 (2004) 024315.
[31] Y. Wang, et al., Phys. Rev. C 67 (2003) 024303.
[32] Y. Wang, et al., Phys. Rev. C 63 (2001) 024309;
J. Äystö, et al., Nucl. Phys. A 480 (1988) 104.
[33] Y. Wang, et al., Chin. Phys. Lett. 23 (2006) 808.
[34] S. Lalkovski, et al., Phys. Rev. C 88 (2013) 024302.
[35] J.A. Sheikh, G.H. Bhat, Y. Sun, R. Palit, Phys. Lett. B 688 (2010) 305.
[36] G.H. Bhat, J.A. Sheikh, R. Palit, Phys. Lett. B 738 (2014) 218.
[37] G.H. Bhat, J.A. Sheikh, R. Palit, Phys. Lett. B 707 (2012) 250.
[38] S. Biswas, et al., arXiv:1608.07840.
[39] C. Zhang, G.H. Bhat, W. Nazarewicz, Y. Shi, Phys. Rev. C 92 (2015) 034307.
[40] J.A. Sheikh, K. Hara, Phys. Rev. Lett. 82 (1999) 3968.
[41] Y. Sun, K. Hara, J.A. Sheikh, J.G. Hirsch, V. Velazquez, M. Guidry, Phys. Rev. C 61 (2000) 064323.
[42] J.A. Sheikh, G.H. Bhat, Y.-X. Liu, F.-Q. Chen, Y. Sun, Phys. Rev. C 84 (2011) 054314.
[43] P. Möller, et al., At. Data Nucl. Data Tables 98 (2012) 149;
https://t2.lanl.gov/nis/data/astro/molnix96/peseps2gamma.html.
[44] S. Akkoyun, et al., Nucl. Instrum. Methods Phys. Res. A 668 (2012) 26;
S. Paschalis, et al., Nucl. Instrum. Methods Phys. Res. A 709 (2013) 44.
[45] M. Vanderbrouck, et al., Nucl. Instrum. Methods Phys. Res. A 812 (2016) 112.
[46] P. Jachimowicz, M. Kowal, J. Skalski, Phys. Rev. C 85 (2012) 034305.
[47] J. Hakala, R. Rodríguez-Guzman, et al., Eur. Phys. J. A47 (2011) 129.
[48] S. Péru, M. Martini, Eur. Phys. J. A50 (2014) 88.
[49] F. Montes, et al., Phys. Rev. C 73 (2006) 035801.